Title: **Task 7c - Worm Tank**

Contributor: **National Research Institute for Earth Sciences and Disaster Prevention**

Date: **March 1998**

CO-ORDINATED RESEARCH PROGRAM ON BENCHMARK STUDY FOR THE SEISMIC ANALYSIS AND TESTING OF WWER-TYPE NUCLEAR POWER PLANTS

Task 7c. Worm Tank

NIED / IHI STUDY:

Part 1

An Experimental Study of the Sloshing Behavior of the Worm Tank

Part 2

An Experimental Study of the Fluid-Structure Interaction Behavior of the Worm Tank

Part 3

A Response Spectrum Analysis of the Worm Tank

March 1998

Prepared by:

National Research Institute for Earth Science and Disaster Prevention

Ishikawajima-Harima Heavy Industries Co., Ltd.

Part 1
An Experimental Study of the Sloshing Behavior of the Worm Tank

Abstract

Worm tank have an unique shape. In the seismic design of the worm tank, it is desirable to clear the behavior of the worm tank under the seismic loading. We assumed that there are two phenomena in the seismic behavior of the worm tank as same as the behavior of the cylindrical and rectangular tanks. One is a sloshing behavior of the water and another is the dynamic response of the worm tank. In this study, we investigate the dynamic characteristics of the worm tank during the strong earthquakes. We conducted the vibration tests to clarify the seismic behaviors of the worm tanks and obtained the valuable data to verify the analytical method.

It was found that the natural frequency can be calculated using the eigenvalue formula of the cylindrical and rectangular tanks. Lower modes of the worm tank are identical with that of the rectangular tank. We can estimate the surface behavior and the impact mode using the data of the rectangular tank.

1 Introduction

There are two phenomena in the seismic behavior of the worm tank as shown in Fig.1. One is a Fluid-Structure Interaction (FSI) mode, and another is a sloshing mode. In this study , we focused on the sloshing of the worm tank. Many studies of vibrational characteristics of the cylindrical and rectangular tank have been published. For example, Kimura 1993 studied the sloshing in the diagonal excitation mode of the rectangular tank and Kobayashi presented the results of the impulsive pressure acting on the roof. However these studies were restrict to the cylinder and rectangular tanks. There are no studies of the vibrational characteristics of the worm tank. In the sloshing mode, it is a point to clarify the natural frequency of the sloshing, the sloshing response, and the impact pressure acting on the roof. Study items in the sloshing analysis of the worm tank are shown in Table 1.

We conducted the sloshing test using a 1/5 scale model of the worm tank. It was conducted at the National Research Institute for Earth Science and Disaster Prevention (NIED), Science and Technology Agency of Japan.

2 Test

We conducted the sloshing tests using a 1/5 scale worm tank model. Tank is partially filled with water. Two different water height were used in the tests. They are 50% and 80% of the tank height. Test conditions are following.

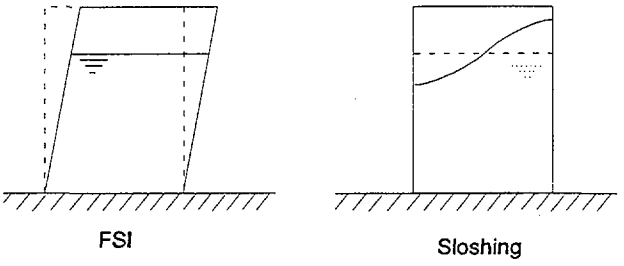

Fig. 1 Vibration Mode of a Tank

2.1 Model

Following are the outline of the worm tank. The shape of the model was shown in Fig. 2.

Long side length: 2600 mm
Short side length: 990 mm
Height : 656 mm
Thickness : 10 mm (Side wall and Roof)
12 mm (Base plate)
Material : acrylic (Side wall ,Roof and Base plate)
: wood (Sheet on the shaking table)

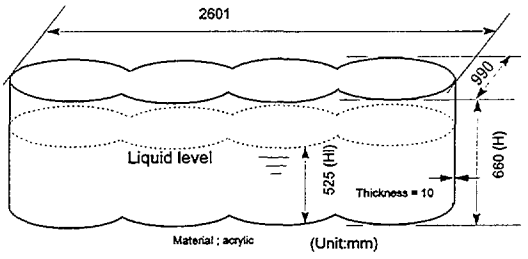

Fig. 2 1/5 Scale Worm Tank Model

2.2 Test case

Test cases are defined to obtain the four basic sloshing characteristics of the worm tank. The model was excited in the short side, the longitudinal and the diagonal directions respectively, as shown in Fig. 3.

(1) Sinusoidal sweep test to get the natural frequencies,

(2) Free vibration test for the damping ratio,

(3) Resonance test for to obtain the resonance response,

and

(4) Seismic response test using El Centro (NS) and JMA-Kobe NS to clarify the pressure impact.

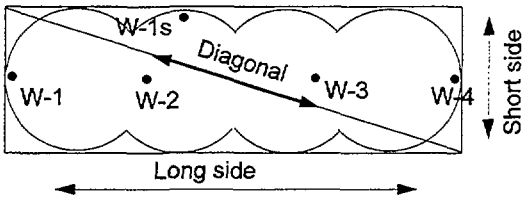

Fig. 3 Direction of the Excitation

Table 1 Study Item for the Seismic Design of the Worm Tank (Sloshing)

Study item	Necessary Data for study	Evaluation Method	Remarks
(1) Seismic Response (Horizontal)	· Natural frequency of FSI	FEM analysis	Verification by experiment
	· Seismic waves · Response spectrum		
(2) Strength of The Side Wall and The Bottom · Strength of The Corner Part · Buckling of The Side Wall	· Dynamic pressure · Overturning moment	FEM analysis	FSI is more important mode
(3) Sliding and Rocking · Sliding · Rocking motion · Up lift of The Bottom Plate · Strength of The Bottom Plate · Effect of The Anchor Bolts	· Overturning moment · Base shear force · Friction between bottom plate and bearing plate	FEM analysis	FSI is more important mode
(4) Strength of The Roof	· Reaction force of piping	FDM	Verification by experiment
(5) Over flow	· Sloshing wave height	FEM, FDM	Verification by experiment
(6) Strength of Nozzle part	· Reaction force of piping	FEM analysis	Experiment is necessary
(7) Effect of reinforcement structure · Wave height	· Detail of reinforcement structure		Experiment is necessary

3.1 Natural frequencies

Natural frequencies which were obtained from the sinusoidal sweep tests are shown in Table 2,3,4 and 5.

These tables also show the analytical natural frequencies of the rectangular tank (the long side is 2600 mm and the short side is 990 mm in length) and the cylindrical tank of which the diameter is 990 mm. The transfer functions are shown in Fig. 4 and 5. In the short side direction, the natural frequencies of the worm tank are between that of the rectangular tank and the cylindrical tank. In the longitudinal direction , the natural frequencies of the worm tank are almost equal to that of the rectangular tank, especially for the lower mode.

Table 2 Natural Frequencies in the Lateral Direction (Unit:Hz) (Hl/H = 0.8)

mode	worm tank	rectangular tank	cylindrical tank
1st	0.90	0.86	0.93
2nd	1.56	1.54	1.64
3rd	2.05	1.99	2.07
4th	2.40	2.35	
5th	2.72	2.66	

Table 3 Natural Frequencies in the Lateral Direction (Unit:Hz) (Hl/H = 0.5)

mode	worm tank	rectangular tank	cylindrical tank
1st	0.86	0.78	0.88
2nd	1.56	1.53	1.63
3rd	2.07	1.98	2.07
4th	2.42	2.35	
5th	2.73	2.66	

Table 4 Natural Frequencies in the Longitudinal Direction (Unit:Hz) (Hl/H = 0.8)

mode	worm tank	rectangular tank
1st	0.44	0.41
2nd	0.96	0.93
3rd	1.21	1.22
4th	1.46	1.45
5th	1.78	1.64

Table 5 Natural Frequencies in the Longitudinal Direction (Unit:Hz) (Hl/H = 0.5)

mode	worm tank	rectangular tank
1st	0.354	0.34
2nd	0.91	0.86
3rd	1.20	1.20
4th	1.46	1.44
5th	1.78	1.64

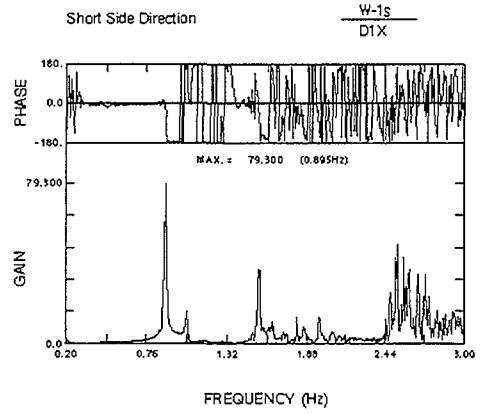

Fig. 4 Transfer Function Spectrum (Lateral)

3.2 Modes in the diagonal excitation

In the rectangular tank, all modes which caused by the horizontal excitation could categorize to the two modes ; one is the longitudinal direction mode and another is the lateral direction mode. So that, when the rectangular tank is shaken in the diagonal direction, we couldn't see any extra modes. The worm tank has complex free surface of the water. It is wondered that there is other modes in the worm tank. Figure 6 shows the transfer function of the input displacement to the liquid height in the diagonal excitation. Table 6 shows the natural frequencies of the diagonal excitation. We can not see any other modes in the diagonal excitation. It is proved that all modes of the worm tank in the horizontal excitation could be categorized to the longitudinal and the lateral modes

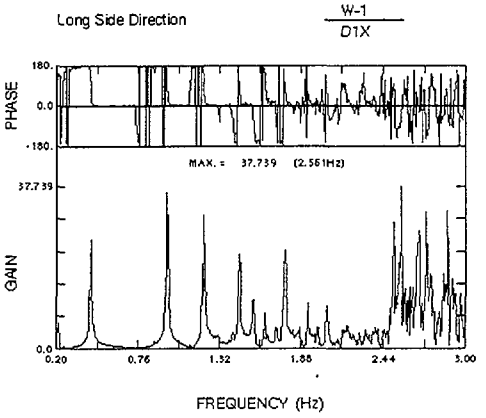

Fig. 5 Transfer Function Spectrum (Longitudinal)

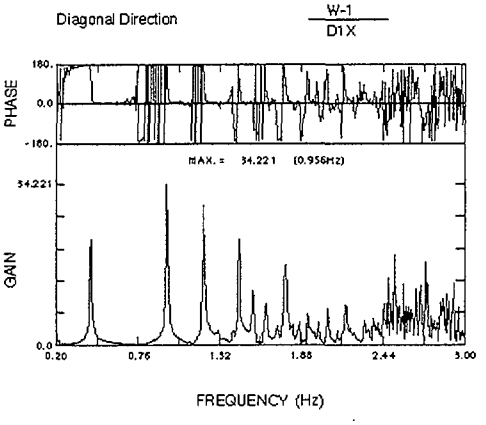

Fig.6 Transfer Function Spectrum (Diagonal)

Table 6 Natural Frequencies in the Diagonal Excitation

(Unit:Hz) (Hl/H = 0.8)

mode	diagonal	longitudinal direction	lateral direction
1	0.44	0.44	
2	0.90		0.90
3	0.96	0.96	
4	1.05		1.05
5	1.21	1.21	
6	1.32	1.32	
7	1.46	1.46	
8	1.56		1.56
9	1.71	1.71	1.71
10	1.78	1.78	

3.3 Damping

The damping ratio of the first, second and third modes are shown in Fig. 7. The damping of the first mode in the longitudinal direction is a little bit high. The damping ratio of the worm tank is a same level as that of the rectangular and the cylindrical tanks.

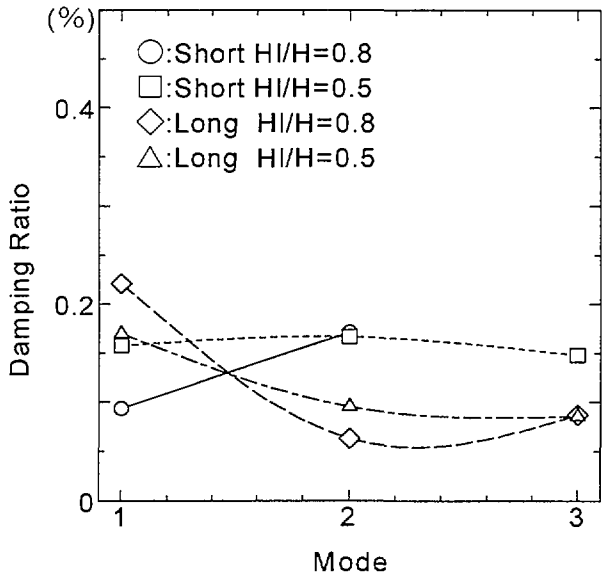

Fig. 7 The Damping Ratio of the Worm Tank

3.4 Response of the resonant excitation

The worm tank was excited by the natural frequency of the each mode. Fig. 8 shows mode amplification. The amplification of the first mode of the longitudinal excitation is lower than that of the lateral mode.

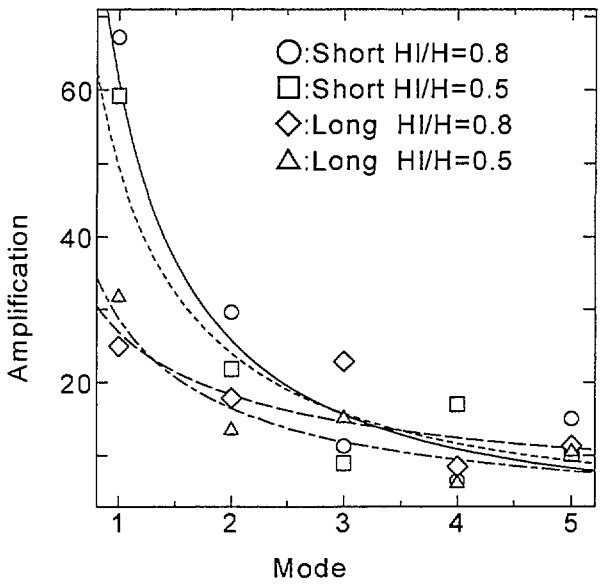

Fig. 8 Mode Amplification

3.5 Seismic response

The impact pressures on the roof is an important factor to the design of the roof. We performed seismic response test which amplitude of 50 gal, 100 gal and 200 gal. The wave height response are shown in table 7. Table 8 shows the impact pressure on the roof in the diagonal, the longitudinal and the lateral modes. El-Centro NS (341 Gal) and JMA-Kobe NS (600 Gal) were used in the excitation.

Table 7 Wave Height in the Seismic Excitation

(Unit:mm)

Excitation level El Centro (NS)		50 Gal	100 Gal	200 Gal
Hl/H=0.8 Lateral	W-1	117.0	impact	---
	W-4	103.8	impact	---
Hl/H=0.8 Longitudinal	W-1	---	impact	impact
	W-4	---	132.3	impact
Hl/H=0.5 Lateral	W-1	80.3	193.8	impact
	W-4	75.0	181.5	impact
Hl/H=0.5 Longitudinal	W-1	---	211.4	impact
	W-4	---	sensor damaged	impact

Table 8 Impact Pressure in the seismic excitation

(Unit:Pa)

Seismic Wave	El-Centro	JMA-Kobe('95.1.17)
Diagonal	8204	8778
Longitudinal direction	8651	10601
Lateral direction	5185	3107

3.6 Slip of the worm tank

The real worm tank is put on the slab and not anchored. The slip of the worm tank is effective to the failure of the worm tank. It is aimed to investigate the sloshing effect to the tank slip. It is true that the less friction coefficient, the easier to slip. Therefor we chose the material of the fluoric polymer and the stainless steel for the sliding surface. The measured friction coefficient is 0.27.

The tests were done only using the earthquake excitation. The seismic wave used in this tests were El-Centro NS and an artificial seismic wave (S2M8PT18). Increasing the amplitude of the excitation wave, we observed the slip of the tank. The excitation direction is both the long side and the lateral direction of the worm tank. The results are shown in Table 9 and Table 10.

Table 9 Slip by the Excitation in the Lateral Direction

(Unit:Gal) (Unit:mm)

Excitation wave	Excitation Level	Result
El-Centro NS	50	no slip
↓	100	↓
↓	150	↓
↓	200	↓
↓	250	↓
↓	300	↓
↓	350	↓
↓	400	17.7 mm
S2M8PT18	300	no slip
↓	500	3.8 mm

Table 10 Slip by the Excitation in the Longitudinal Direction (Unit:Gal) (Unit:mm)

Excitation wave	Excitation Level	Results
El-Centro NS	100	no slip
↓	200	↓
↓	300	↓
↓	400	↓
↓	500	↓
S2M8PT18	500	↓
↓	600	↓
↓	800	↓
↓	1000	7.3

4 Discussion

4.1 Natural Frequencies

We can solve analytically the natural frequency in the sloshing mode of the cylindrical and the rectangular tank. The analytical solution of the natural frequency of the cylindrical tank and the rectangular tank are as follows;

cylindrical tank: $$f_n=\frac{1}{2\pi}\sqrt{J_{1n}\, g\, \tanh(J_{1n}\frac{hl}{R})/R}$$

rectangular tank: $$f_{im}=\frac{1}{2\pi}\sqrt{\frac{(2m-1)\pi g}{L}\tanh\frac{(2m-1)\pi h}{L}}$$

Usually, we use FEM analysis for any other shaped tanks. However, it is found that the fundamental mode of the worm tank in the long side direction is identical with that of the the rectangular tank and the frequency in the lateral direction is identical with that of the cylindrical tank. So we can get the natural frequency of the worm tank without FEM analysis.

4.2 Mode

The lower two modes of the worm tank both in the longitudinal and the lateral mode are similar with that of the rectangular tank. The modes above second mode is complex shapes which combined the modes of a cylindrical and a rectanguler tank. There are many modes that couldn't be excited by the sweep test. Because these modes have very small participation factors for the long side and the lateral direction excitation. Those modes couldn't be excited well by the small level excitation.

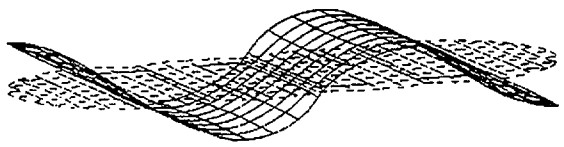

Fig. 9 third mode of water surface

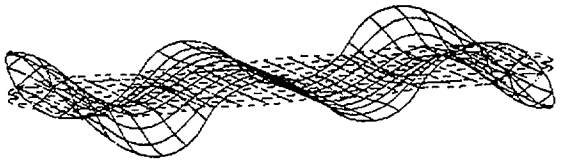

Fig. 10 fifth mode of water surface

However it was found that these modes would be appeared by the stimulating the water surface like the roof impact. Our target modes were third and fifth modes that are shown in Fig. 9 and 10. we could excite the fifth mode with sinusoidal wave. The fifth mode were observed every in the diagonal, the long side and lateral excitation. This mode never be excited without the roof impact. All modes could be possibly excited by the large amplitude excitation such as a seismic loading.

4.3 Damping

The worm tank have three necks in the long side direction. The damping ratio of the first mode is a little bit high at the 80% water level. That value are not different from those of the rectangular and the cylindrical tanks respectively. It is supposed that the shape of the worm tank is not effective on the damping ratio.

4.4 Response Amplitude

The amplification of the first mode of the lateral excitation is twice larger than that of the long side mode as shown in Fig. 8. It means that the worm tank is sensitive to the lateral excitation.

4.5 Roof impact

When diagonal exciting with El-Centro wave, the maximum impact pressure observed at P601, and when longitudinal excite with El-Centro wave, the maximum impact pressure observed at P303. These result means that asymmetrical mode was excited in the test. It was fifth mode as mentioned above. From the observation of these tests, second mode of the long side direction was well excited in the El-Centro wave, while JMA-Kobe wave well excited the first mode. The distributions of the impact pressure in the lateral direction of the El-Centro wave are not similar that of the JMA-Kobe as shown in Fig. 11.

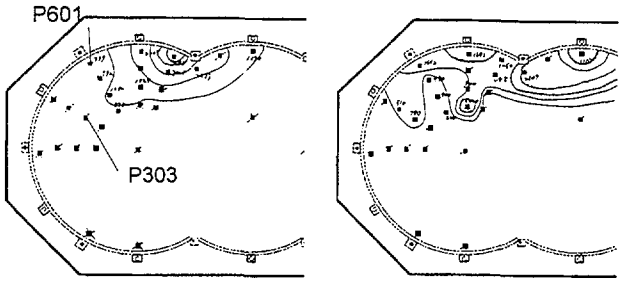

Fig. 11 Impact Pressure Distribution on the Roof

4.6 Slip of the worm tank

The condition of tank slip is explained by next equation. The mass "m" is not equal to the total tank mass of the liquid storage tank. If all of the acceleration is directly transfer to the containment liquid, the slip shall be occurred at 270 Gal. However, the liquid absorbs the excitation energy by transforming.

The slip occurred at 400 gal El-Centro Wave in the lateral

$$\mu N \leq F_{slide} = ma$$

μ ; *Friction coefficient*
m ; *mass*
a ; *acceleration*

direction. On the other hand, the slip dose not occurred under 500 gal in the long side excitation. In the S2M8PT18 wave, the slip occurred at the 500 gal in the short side excitation and 1000 gal in the long side excitation. It was found that the slip in the short side direction will occur easily than that of the long side excitation.

Usualy, when the most of the liquid move toward the inverse of the acceleration, the tank will slip at the low level excitation. This is the sloshing effect on the tank slip. But it is not observed in this test using the El-Centro wave and S2M8PT18 wave.

5 Conclusions

The sloshing characteristics of the worm tank were investigated. The results are as follows:

1. The natural frequency of the worm tank can be calculated using the formula of the frequency of a cylindrical tank or a rectangular tank. Lower modes are identical with that of the rectangular tank.
2. It is possible to estimate the surface behavior and the impact mode using that of the rectangular tank.
3. In the lateral excitation, the slip of the worm tank occurred and the amplitude of the response in the seismic excitation is twice than that of the longitudinal excitation.

References

Abramson and Norman H.,1966, "The Dynamic Behavior of Liquids in Moving Containers," NASA SP-106

Kimura K.,Takahara H.,and Sakata M.,1993,"Sloshing in a Rigid Tank Subjected to Pitching Excitation," JSME C-59 565 14

Kobayashi N. "Impulsive Pressure Acting on the Tank Roofs caused by Sloshing Liquid," Proceeding of 7th WCEE

Part 2
An Experimental Study of the Fluid-Structure Interaction Behavior of the Worm Tank

Abstract

In the seismic design of the worm tank, it is desirable to clear the behavior of the worm tank under seismic loading. We assumed that there are two phenomena regarding seismic behavior of the worm tank, being the same behaviors of cylindrical or rectangular tanks. One is the sloshing behavior of the water and the other is fluid structure interaction (FSI) response of the tank itself. In a previous study report[1], we reported the sloshing behavior of the worm tank. We conducted vibration tests and obtained valuable data to clarify the sloshing behavior and verify the analytical method. In this paper we will present the results of the FSI test. We performed the FSI test using a one-third size steel worm tank model. We utilized a simulation analysis using the finite element computer code. We found the characteristics of the FSI response modes. The concentration of stress occurred near the columns of the longitudinal side wall, and acceleration in the lateral direction was ten times larger than that of the longitudinal direction.

1 Introduction

There are two phenomena in the seismic behavior of the worm tank. One is the fluid-structure interaction (FSI) mode, and the other is the sloshing mode as shown in Fig.1. Many studies of the vibrational characteristics of cylindrical and rectangular tanks have been published. However, such studies were restricted to cylinder and rectangular tanks[2],[3],[4]. There are no studies on the vibrational characteristics of the worm tank. As a first step, we conducted sloshing tests and reported the sloshing behavior of the worm tank[1]. As the second step, we made a one-third scale steel model and performed FSI tests. This is a report on the results of that testing. The tests were performed at the National Research Institute for Earth Science and Disaster Prevention (NIED) of the Science and Technology Agency (STA) of Japan, in cooperation with Ishikawajima -Harima Heavy Industries Co., Ltd. (IHI), and under the supervision of Prof. H. Shibata of Yokohama National University. The worm tank has an unique shape. So it is not easy to predict its seismic behaviors. The objective of this study is to investigate the dynamic behavior of a worm tank during strong earthquakes. Vibration tests are very important to clarify the seismic behaviors of the worm tank and to verify analytical methods. We performed a computer simulation using the finite element method.

2 Fluid-Structure Interaction (FSI) Mode

In the FSI mode, the strengths of the side wall and base plate are the most important factors to clarify. The items to be studied are listed in Table 1.

3 Test

We conducted the FSI testing using a 1/3-scale steel worm tank model and a large shaking table. The model was set on and not fixed to the shaking table. Test conditions are listed in the following.

3.1 Model

The shape of the model is shown in Fig. 2. The thickness of the wall plate was chosen to be one-third that of the actual tank. Six columns and tie-rods are used to reinforced the side wall, as same as an actual tank. The structure of the worm tank is shown in Fig.3.

Length (longitudinal direction)	: 5,323.2 mm
Length (lateral direction)	: 2,122 mm
Height	: 1,286 mm
Thickness	: 1.6 mm (main body, Roof)
	: 3.2 mm (Base plate)
material	: steel (SS400)

3.2 Measurement

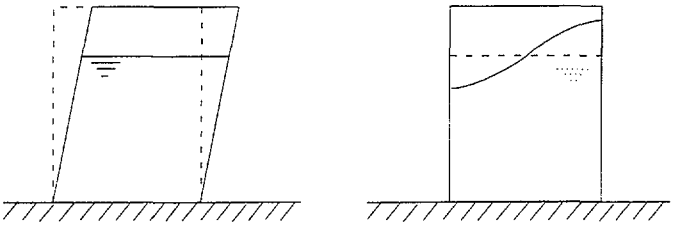

Fig. 1 Vibration Mode of a Tank

Acceleration:	20 ch (shaking table, base plate,side wall and roof.)
Pressure	: 30 ch (sidewall and roof)
Strain	:134 ch (sidewall, roof and base)

Table 1 Study Item for Seismic Design of Worm Tank (FSI Mode)

Study item	Necessary Data for study	Evaluation Method	Remarks
(1) Seismic Response (Horizontal, Vertical)	· Natural frequency of FSI	FEM analysis	Verification by experiment
	· Seismic waves, response spectrum		
(2) Strength of side wall and bottom · Strength of Corner part · Buckling of side wall	· Dynamic pressure · Overturning moment	FEM analysis	Verification by experiment
(3) Sliding and rocking · Sliding of tank · Rocking motion · Up lift of bottom plate · Strength of bottom plate · Effect of anchor	· Overturning moment · Base shear force · Friction between bottom plate and bearing plate	FEM analysis	
(4) Strength of nozzle attachment part	· Reaction force of piping	FEM analysis	
(5) Effect of reinforcement Structure	· Detail of reinforcement structure		Experiment

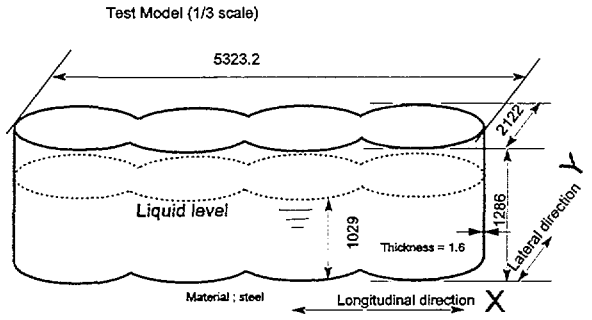

Fig. 2 1/3 Scale Worm Tank Model

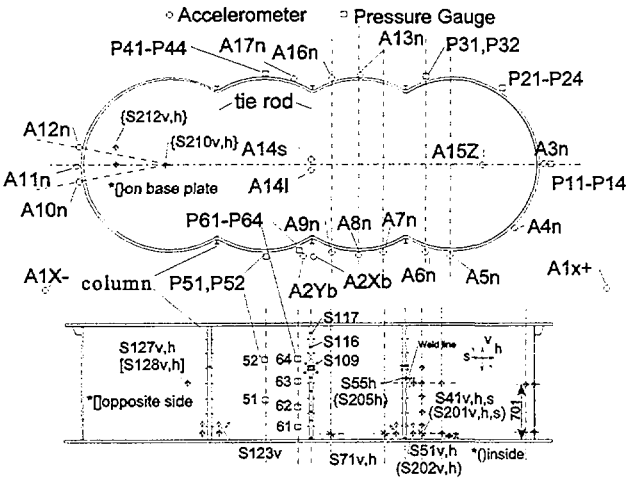

Fig.3 Position of Sensors

3.3 Test case

Test cases were planed to obtain three basic characteristics of FSI. The worm tank was excited in the longitudinal and lateral directions, and the following tests performed:

(1) Sinusoidal sweep test to get natural frequencies.

(2) Resonant response test to obtain the resonant response.

(3) Seismic response test using Paks wave and El_Centro (NS) wave.

4 Test Results

4.1 Natural frequencies

The natural frequencies of the worm tank were extracted from the transfer function of the sinusoidal sweep test. The excitation was done both in the longitudinal and lateral

directions. The acceleration transfer functions in the lateral direction are shown in Fig.4 and those of the longitudinal direction are shown in Fig.5. We could not find any peak in the range from 2.0 to 10.0 Hz. The spectra in the frequency range from 10.0 to 30.0 Hz are shown. Natural frequencies of the major peak from those spectra are listed in Table 2.

Table 2 Natural Frequencies

No.	Lateral direction	Longitudinal direction
	Frequency (Hz)	Frequency (Hz)
1	11.7	14.01
2	16.7	17.2
3	19.5	20.9
4	20.6	23.0
5	21.1	23.5
6	22.8	24.4

4.2 Resonant response

Tables 3 and 4 are lists of the maximum response values under the sinusoidal wave of the resonant frequency. The amplitude of the response in the lateral direction becomes large. The amplitude of the input wave was suppressed to 30 gal, while that in the longitudinal direction was 50 gal. The ratio of response to input acceleration is nearly 10 in the lateral direction, while that in the longitudinal direction is 60. This means that earthquake in the lateral direction would be more severe to a worm tank.

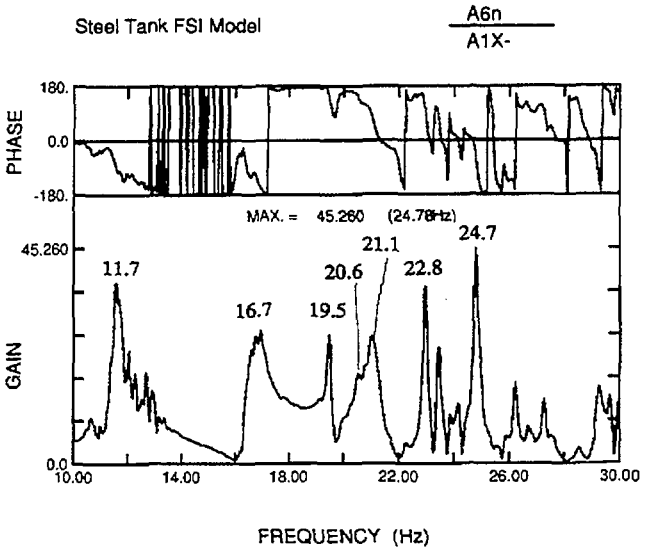

Fig.4 Transfer Function Spectrum (lateral)

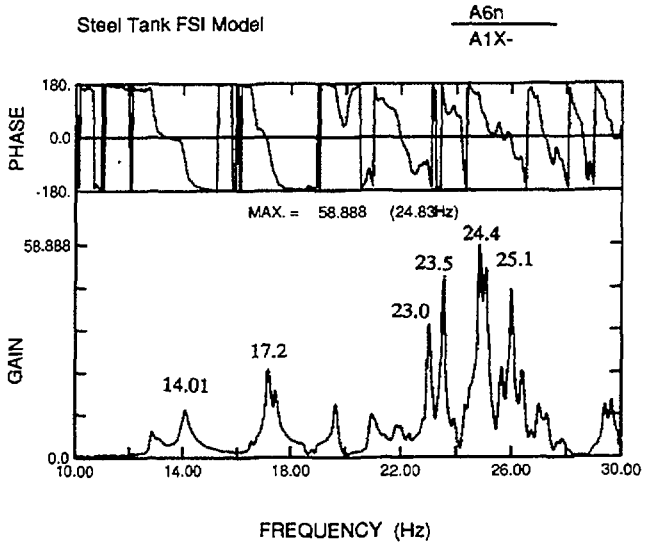

Fig.5 Transfer Function Spectrum (longitudinal)

Table 3 Resonant Response (Lateral Direction)
(input:30 gal)

No.	Frequency (Hz)	Max. acceleration (gal)
1	16.7	2939 (A10n)
2	19.5	2688 (A13n)
3	20.6	-2251 (A7n)
4	21.1	-2251 (A7n)
5	22.8	-1823 (A7n)
6	29.8	2620 (A7n)

Table 4 Resonant Response (Longitudinal Direction)
(input:50 gal)

No.	Frequency (Hz)	Max. Acceleration (gal)
1	14.0	1317 (A7n)
2	17.2	1224 (A7n)
3	23.0	-2167 (A7n)
4	24.4	1788 (A3n)
5	24.8	2696 (A7n)
6	25.1	2562 (A6n)

4-3 Seismic response

We used three kinds of seismic waves. We used the time history of the seismic wave in the Paks NPP: "PAKS 793X" and "PAKS 793Y". Y means the longitudinal direction and X means lateral direction of the tank. All of the wave shapes (time compressed) are shown in Fig. 6.

Here, we present the results of the floor response wave (PAKS793Y in the lateral direction and PAKS793X in the longitudinal direction) and El_Centro wave. PAKS 793X and Y are the seismic waves in the actual plant site. El_Centro wave does not have a higher power peak in the frequency range, as shown in Figs. 7, 8 and 9. Tables 5, 6, 7 and 8 show the five largest measured values of the acceleration, dynamic pressure and stress. The time histories of these data are shown in Figs. 10, 11, 12 and 13.

4.4 Numerical simulation results

We had conducted a pre-analysis to clarify the fundamental FSI mode of the test model. We used the general-purpose FEM code ANSYS. Figure 14 shows an FEM model of the worm tank. The results are shown in Fig. 15. Natural frequencies and participation factors of each mode are listed in Table 9. The anti-symmetrical modes of the tank axis have a large participation factor. From these results, we assumed that three major modes below 20 Hz are sensitive to the excitation. These results were used to design the test model and for the response spectrum analysis.

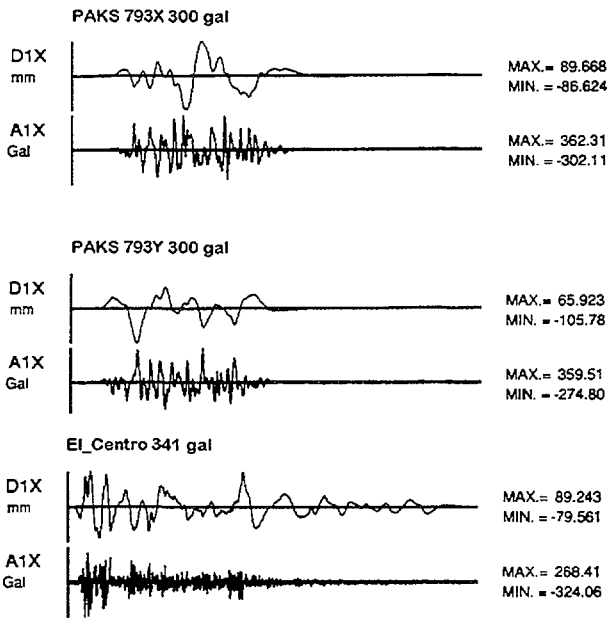

Fig.6 Time History of the Seismic Wave

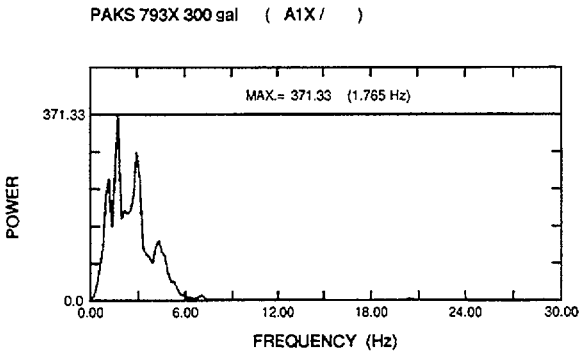

Fig.7 Power Spectrum of PAKS 793X

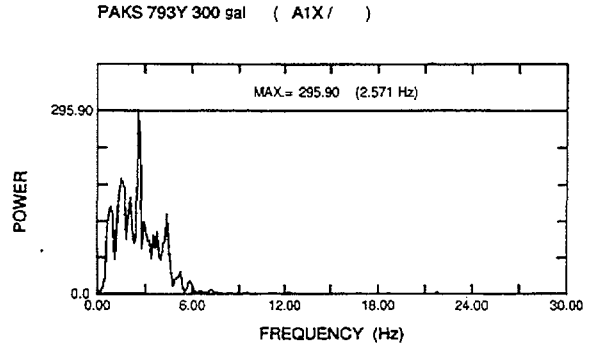

Fig.8 Power Spectrum of PAKS 793Y

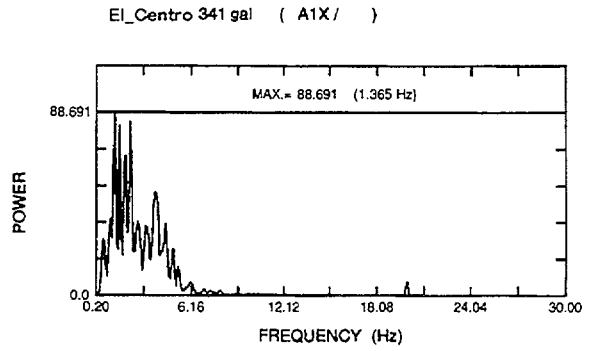

Fig.9 Power Spectrum of El_Centro (NS)

Table 5 Seismic Response of PAKS 793Y (300 gal) (Lateral Direction)

Rank	Acceleration (gal)	Dynamic pressure (Pa)	Stress (kgf/mm^2)
1	4846 (A13n)	7441 (P44)	3.43 (S201v)
2	2961 (A9n)	7057 (P64)	-3.22 (S109v)
3	2749 (A7n)	6705 (P52)	2.97 (S41v)
4	2597 (A8n)	5246 (P32)	-2.90 (S128v)
5	2505 (A5n)	4984 (P31)	2.68 (S205h)

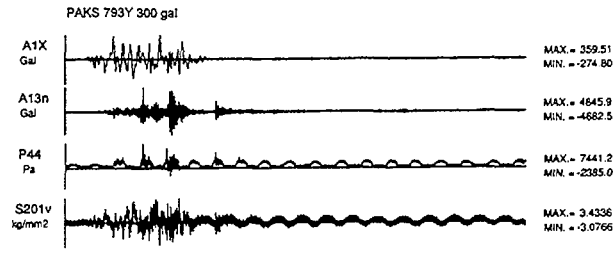

Fig.10 Seismic Response of PAKS 793Y (Lateral Direction)

Table 6 Seismic Response of PAKS 793X (300 gal) (Longitudinal Direction)

Rank	Acceleration (gal)	Dynamic pressure (Pa)	Stress (kgf/mm^2)
1	-498 (A10n)	3895 (P11)	-5.44 (S123v)
2	-492 (A11n)	3639 (P12)	3.85 (S212s)
3	476 (A3n)	3351 (P21)	-3.53 (S51h)
4	-436 (A12n)	2863 (P22)	2.23 (S117-)
5	-398 (A7n)	2860 (P14)	1.86 (S116-)

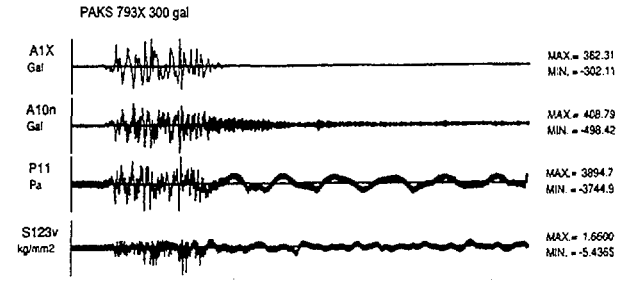

Fig.11 Seismic Response of PAKS 793X (Longitudinal Direction)

Table 7 Seismic Response of El_Centro (341 gal) (Lateral Direction)

Rank	Acceleration (gal)	Dynamic pressure (Pa)	Stress (kgf/mm^2)
1	-1364 (A13n)	3378 (P32)	-13.1 (S51h)
2	-814 (A9n)	-3255 (P31)	9.57 (S51v)
3	-740 (A7n)	2942 (P42)	-4.60 (S128v)
4	718 (A6n)	2932 (P41)	3.54 (S212s)
5	-622 (A8n)	2631 (P21)	-2.86 (S71v)

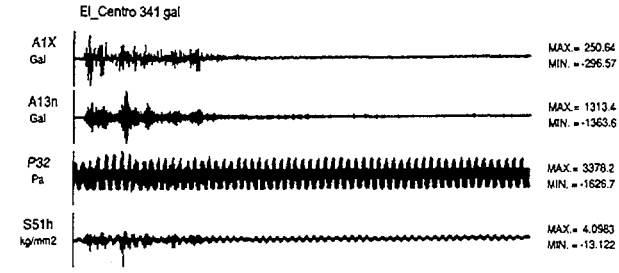

Fig.12 Seismic Response of El_Centro (NS) (Lateral Direction)

Table 8 Seismic Response of El_Centro (341 gal) (Longitudinal Direction)

Rank	Acceleration (ga	Dynamic pressure (Pa)	Stress (kgf/mm^2)
1	-397 (A11n)	-3040 (P11)	3.44 (S212s)
2	-370 (A3n)	-2660 (P21)	2.32 (S117-)
3	354 (A12n)	-2611 (P13)	1.89 (S116-)
4	-341 (A10n)	-2572 (P12)	1.79 (S117+)
5	275 (A7n)	2384 (P22)	1.57 (S210l)

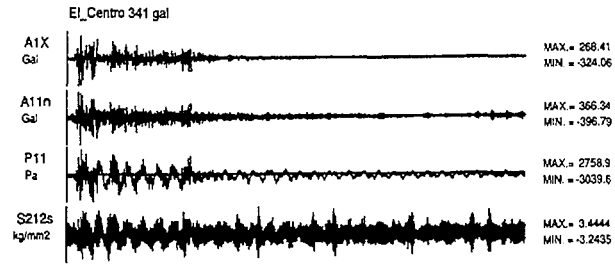

Fig.13 Seismic Response of El_Centro (NS) (Longitudinal Direction)

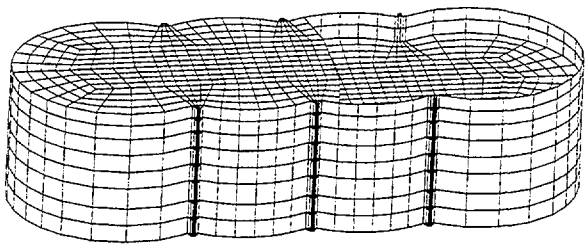

Fig.14 Worm Tank FEM Analysis Model

5 Response spectrum analysis

We conducted the response spectrum analysis. The spectrum produced by Siemens is used. It was shown in Fig.16. The distribution of the stress are shown in Fig.17 and Fig.18.

Table 9 FEM Analysis Results

Mode	Natural frequency (Hz)			Participation factor	
	Test	Analysis		X	Y
		1/3 Scale	Real Scale		
1		10.82	2.12	-6.59-06	2.78e-09
	14.0X	15.27	4.81	1.85-07	-6.49e-03
3	16.7 Y	15.56	4.95	-4.16-09	-7.55e-06
4		19.06	5.95	4.81-08	-7.63e-05
5	17.2X	19.14	6.13	-5.47-03	5.25e-09
6	19.5X	19.46	6.89	-1.54-02	1.70 -08

5 Discussion

5.1 Natural frequency

The results of the FEM analysis and test are listed in Table 9. As shown, the results of the FEM analysis are in good agreement with those of the tests. It was found that these results have more errors in the lower modes, because of the uncertain peaks shown in Fig. 4. But it was still possible to estimate the mode frequency. Worm tank had six columns and six tie-rods to reinforced the connection of cylinder parts. The column restrained the vibration of the side wall. So, the maximum stress appeared near the columns.

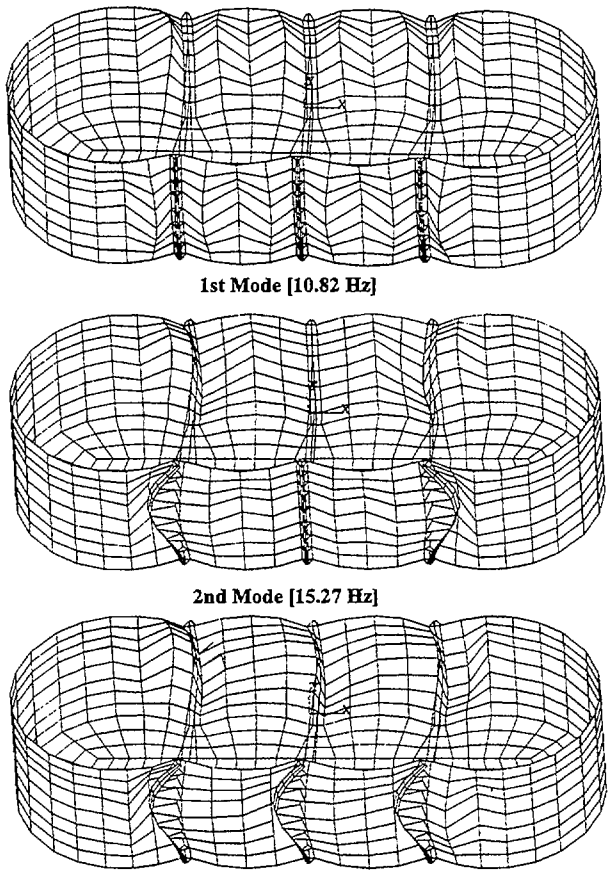

1st Mode [10.82 Hz]

2nd Mode [15.27 Hz]

3rd Mode [15.56 Hz]

Fig.15 Mode of Worm Tank

5.2 Response spectrum analysis

The stress by extension in the lateral direction is larger than that in the longitudinal direction. The maximum stress appeared near the outside column in both cases.

5.3 Seismic response

In the seismic response test, response in the lateral direction is more severe than that in the longitudinal direction, while in the sloshing behavior as presented in [1], longitudinal excitation was more severe than that in the lateral direction. Although the tank was not fixed to the table floor by anchor bolts, the tank did not slip or overturn. Acceleration and pressure in the lateral excitation are larger than those of the longitudinal direction in Paks wave. Stress in the lateral excitation is larger than that of longitudinal excitation in El_Centro wave.

4 Buckling

The worm tank buckled at the side wall. We could not certify the test case of buckling. Figure 19 shows the location of buckling. A crack appeared near the buckling part. Since there were few sensors attached around this area, we could not obtain acceleration, dynamic pressure and strain information from the data. We

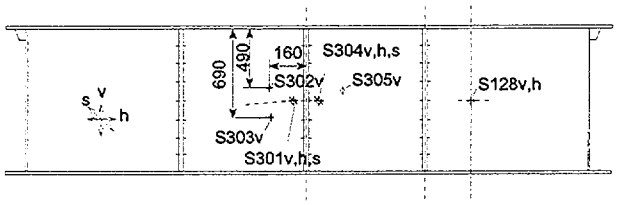

Fig.19 Placement of Buckling

suppose that it was caused by residual stress of the welding and the initial strain under fabrication. Because the wall thickness of model tank is too thin, buckling of the thin-walled structure is often observed. This buckling is not essential to the worm tank.

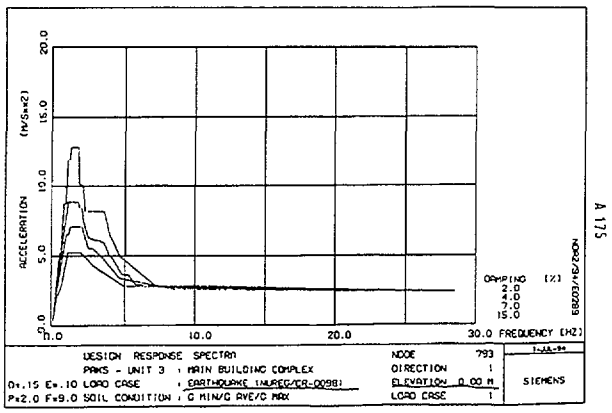

Fig.16 Design Spectra of Paks NPP

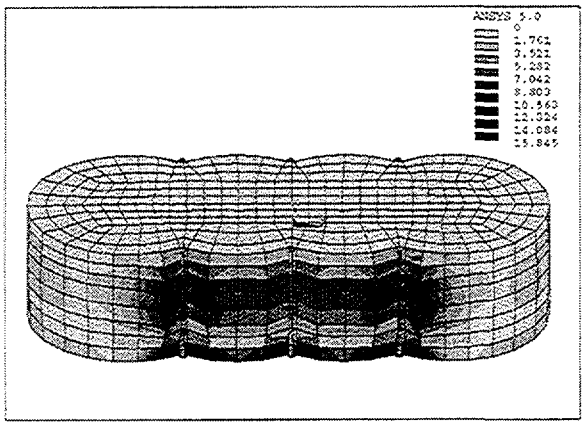

Fig.17 Stress Distribution (Lateral Direction)

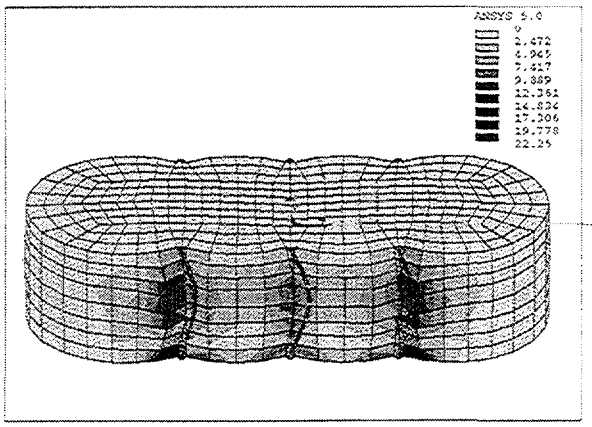

Fig.18 Stress Distribution (Longitudinal Direction)

Conclusion

The FSI characteristics of the worm tank were investigated. The results are as follows;

- FSI behavior appeared apparently in the vibration of the worm tank.
- Acceleration in the lateral excitation is ten times larger than that in the longitudinal excitation during Paks wave excitation.
- In special cases such as resonant response, the amplitude of the response is about 100 times.
- Overturning was not observed under 300 gal of seismic excitation.
- Slip between the I-beam and wooden base plate was not observed.

Acknowledgment

The authors are grateful to Dr. N. Krutzik of Siemens in Germany for his presentation of the Paks NPP earthquake data and Dr. T. Katona of Paks NPP in Hungary for his discussion and nice advise for our test.

REFERENCES

[1] N. Ogawa, T. Chiba, S. Nakajima, H. Shibata, and D. C. Ma, "An Experimental Study of the Sloshing Behavior of the Worm Tank", ASME PVP-Vol.337 141, 1996.

[2] C. Minowa, N. Ogawa, I. Harada, and D. C. Ma, "Sloshing Roof Impact Tests of a Rectangular Tank" ASME PVP-Vol.272 13, 1994.

[3] K. Kimura, H. Takahara, and M. Sakata, "Sloshing in a Rigid Tank Subjected to Pitching Excitation",JSME C-59 565 14, (Japanese).

[4] Abramson and H. Norman, "The Dynamic Behavior of Liquids in Moving Containers", NASA SP-106, 1966.

Part 3
A RESPONSE SPECTRUM ANALYSIS OF THE WORM TANK

ABSTRACT

As a part of a series of tests and analyses for proving the seismic qualification of the worm tank, response spectrum analyses were conducted. We conducted vibration tests to clarify the dynamic characteristics of the worm tank in 1995 and 1996. From the results of these tests, it found that the finite element method is an useful tool to estimate the dynamic behavior of the worm tank. We performed a seismic analysis of an actual worm tank using the finite element method. In this report, we present the results of our analysis. We found that the frequency range of the sloshing and bulging modes of the worm tank are out of the peak range of the design spectrum of the worm tank. The worm tank is not sensitive to earthquakes.

INTRODUCTION

International community places a big emphasis on the problem of seismic qualifications of the WWER-type NPP in Eastern Europe. One of the important and complicated safety-related systems of these NPPs is the worm tank. Damage to the worm tank induces cracking in the lower part of the side wall and in the sides of the columns, leading to serious leakage of water. The worm tank has an unique shape. It is not so easy to predict its seismic behavior. There are no studies on the vibrational characteristics of the worm tank. We performed vibration tests to study the dynamic characteristics of the worm tank in 1995 and 1996. In the first step, we conducted sloshing tests and reported the sloshing behavior of the worm tank. As the second step, we performed fluid-structure interaction (FSI) tests using a one-third scale steel model. We found the characteristics of the FSI response modes. The stress concentrated near the columns of the longitudinal side wall. The acceleration in lateral excitation was larger than that of longitudinal excitation. From the results of the above tests, it was found that the FEM method is an useful tool to estimate the dynamic behavior of the worm tank. The objectives of this study are to investigate the dynamic behavior of an actual worm tank during strong earthquakes. We performed a seismic analysis of an actual worm tank using the FEM. We used the worm tank and the design spectrum of Paks NPP in Hungary as an analytical model. It was found that the frequencies of the sloshing and bulging modes were out of the peak range of the design spectrum . It was also found that an earthquake is not so severe in terms of causing stress to a worm tank.

ANALYSIS

We conducted a stress analysis , free vibration analysis and response spectrum analysis to clarify the dynamic behavior of the actual worm tank.

Model

We used the worm tank of the Paks NPP in Hungary. The following is an outline of the worm tank. A schematic of the worm tank is shown in Fig. 1. Six columns supported and reinforced the side wall. Columns were connected with two tie-rod each other. Upper and lower tie-rod were used to prevent the deflection of the columns.

Length: 15,900 mm
Width : 5,590 mm
Height: 3,857 mm
Water Height: 3,080 mm
Thickness of the side wall: 6,5, and 4 mm (lower, middle and upper)
Material: Stainless Steel
Allowable stress: 21 kgf/mm^2

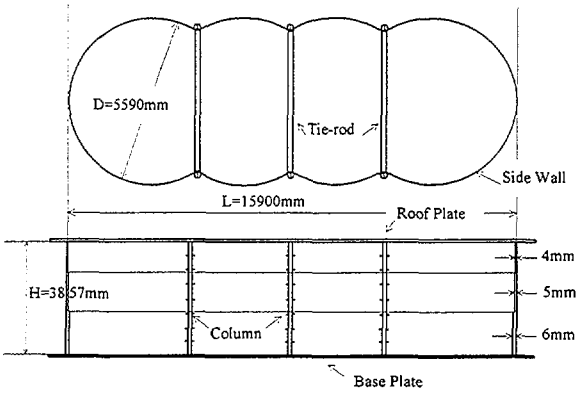

Fig.1 A Schematic of the Worm Tank

Finite Element Analysis

We used a 3-D finite element model of the worm tank using computer program ANSYS. The tank is modeled by means of the shell element, water by the solid element and tie-rod by the beam element.

The tank was fixed at the bottom. To represent the circumferential modes clearly, the circumferential mesh of the shell was set to "small" as shown in Fig.2.

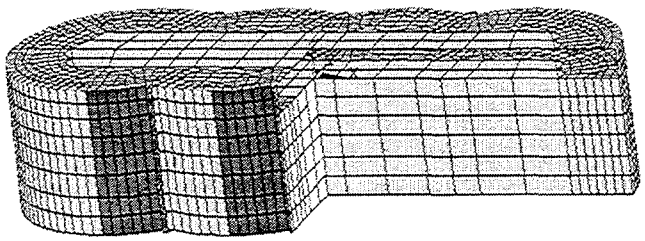

Fig.2 3-D Worm Tank Model

Linear Static Analysis

In the case that the wall plate is thin, the stress caused by water pressure is not negligible small. We conducted a stress analysis of the worm tank under water pressure.

Free Vibration Analysis

To calculate and check the frequency range of the worm tank, we conducted a free vibration analysis. The effect of water pressure on the vibration of the worm tank is considered in this analysis. The effect of water on the vibration of the tie-rod in water was not considered. We calculated the frequencies and modes of the sloshing and bulging modes.

Response Spectrum Analysis

Analysis of the horizontal excitation was done but not that of vertical excitation. We have calculated the stress of the worm tank in the bulging mode but not in the sloshing mode. The design spectrum which was calculated by Siemense was used. Damping is 2%.

RESULTS

Stress under water pressure

The distributions of hoop stress in the side wall are shown in Fig.4. The stress at the lower part of the side wall is larger and is the same level as that for the formula of a cylinder. The stress near the columns is smaller than that of the side wall.

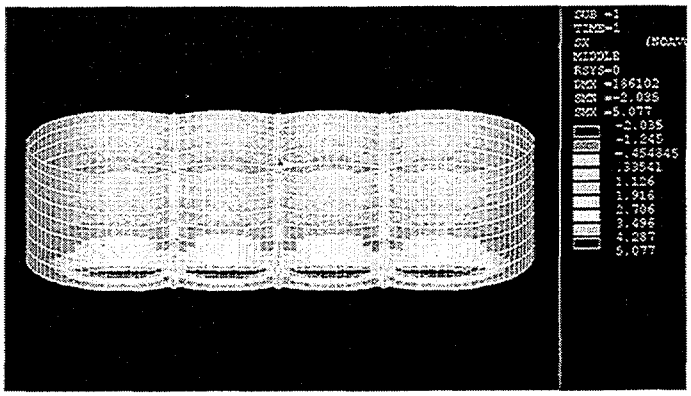

Fig.3 Distribution of the Hoop Stress under Water Pressure

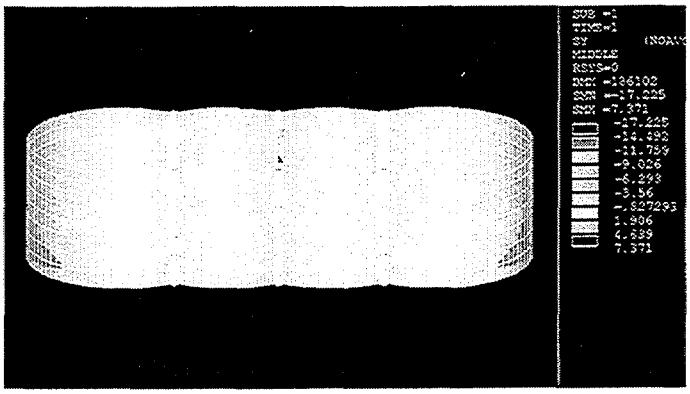

Fig.4 Distribution of the Axial Stress under Water Pressure

Frequencies and Modes

We got 30 frequencies and modes under 20 Hz in the bulging mode. 1st mode is dominant in longitudinal excitation and 7th mode is dominant in lateral excitation. The frequencies and participation factors of the bulging and sloshing mode are listed in Table 1. Typical modes of bulging are shown in Figs.5 and 6. The modes of the tie-rod were observed in the low frequency range as shown in Figs.7. The vibration modes of side wall are observed in Fig. 8. The side wall – tie-rod interaction were observed in the low frequency modes.

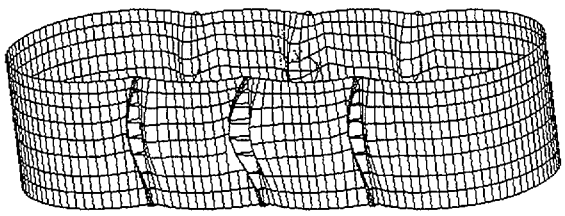

Fig.5 1st Mode of Bulging

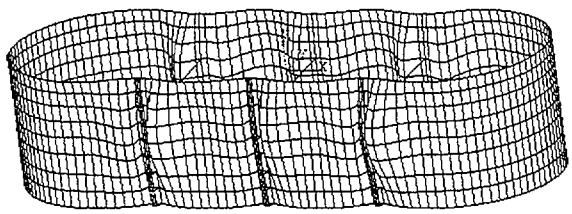

Fig.6 7th Mode of Bulging

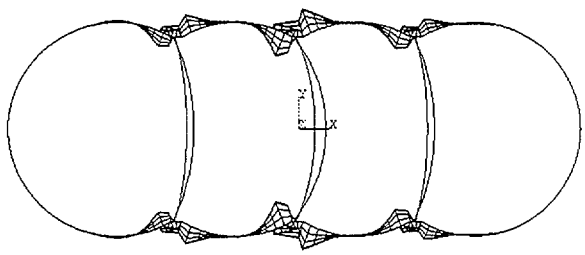

Fig. 7 Vibration Mode of Tie-Rod (1st Mode)

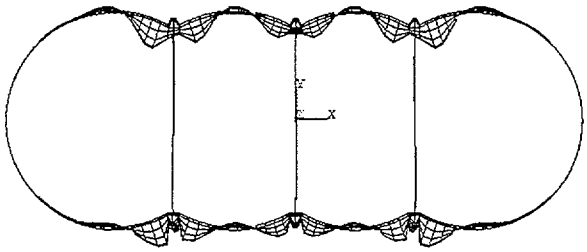

Fig.8 Vibration Mode of Side wall (7th Mode)

Deformations

During both longitudinal and lateral excitation, torsion of the column appeared. The mode in the longitudinal excitation is shown in Fig.9 and that of lateral excitation in Fig.10 . In the longitudinal excitation , vibration of a tie-rod induced to the torsion of the column. In the lateral excitation, the outward deformation of the side wall induced to the bending of the column.

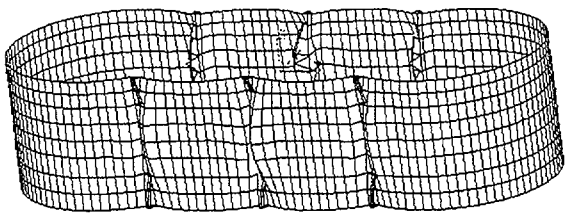

Fig.9 Deflection in Longitudinal Excitation

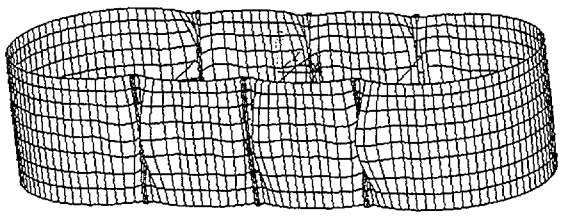

Fig.10 Deflection in Lateral Excitation

Table 1 Frequencies and Participation Factors of Actual Worm Tank

	Bulging Mode				Sloshing Mode		
		Longitudinal Direction		Lateral Direction		Vertical Direction	
Mode	Frequency (Hz)	Participation Factor	Ratio	Participation Factor	Ratio	Frequency (Hz)	Participation Factor	Ratio
1	5.988	-8.47E-01	1.000	-4.78E-06	0.000	0.055	2.22E-09	1.000
2	6.336	-3.68E-04	0.000	-6.36E-06	0.000	0.094	1.14E-10	0.051
3	7.868	2.02E-01	0.238	4.49E-06	0.000	0.115	8.75E-11	0.039
4	8.014	-3.55E-06	0.000	5.22E-05	0.000	0.121	1.65E-10	0.074
5	8.219	-8.94E-07	0.000	-2.69E-01	0.097	0.122	-6.69E-11	0.030
6	8.804	-1.71E-06	0.000	1.91E-04	0.000	0.133	-7.02E-11	0.032
7	9.620	1.89E-06	0.000	-2.77E+00	1.000	0.141	1.98E-10	0.089
8	9.952	1.12E-06	0.000	-7.97E-04	0.000	0.146	1.19E-10	0.054
9	10.102	-2.99E-07	0.000	-4.99E-01	0.180	0.153	1.55E-10	0.070
10	15.130	3.53E-04	0.000	1.63E-05	0.000	0.161	-7.98E-11	0.036

Stress in the seismic excitation

In the seismic analysis, the stress concentrated near the columns. In the longitudinal excitation Maximum stress caused by the vibration of the tie-rod was observed at the joint of the column and this is larger than that of the side wall. In the lateral excitation, maximum stress was observed at the side of the column. The distribution of the hoop stress in longitudinal excitation shown in Fig.11, and the distribution of the lateral excitation in Fig.12. The stress distributions of axial stress were shown in Figs. 13 and 14. Both distributions have the same behavior.

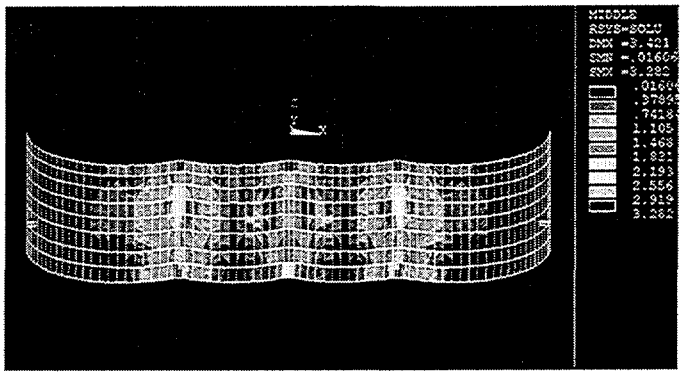

Fig.12 Hoop Stress in the Lateral Excitation

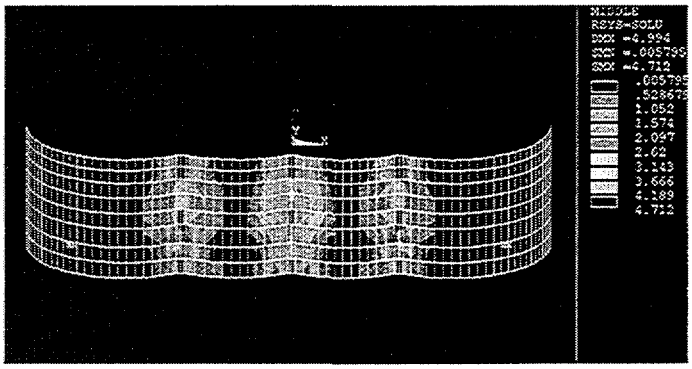

Fig.11 Hoop Stress in the Longitudinal Excitation

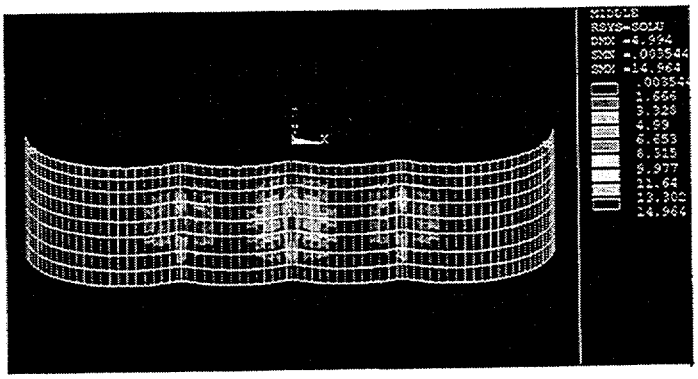

Fig.13 Axial Stress in the Longitudinal Excitation

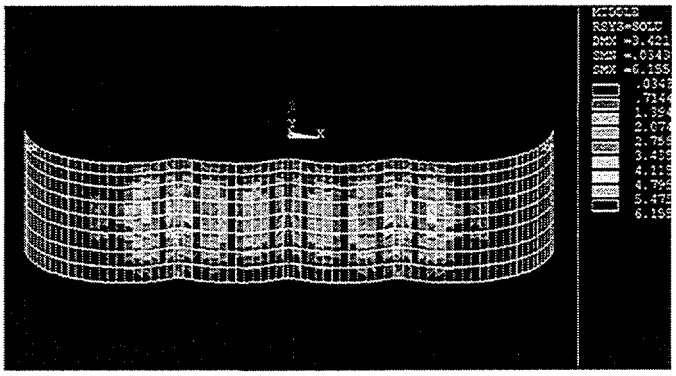

Fig.14 Axial Stress in the Lateral Excitation

DISCUSSION

Design Spectrum and Frequencies of the Worm Tank

The frequencies of the sloshing and bulging modes are out of the peak range of the design spectrum as shown in Fig. 15 . So the amplitude of the displacement and the stress of the worm tank do not become large. It was found that an earthquake is not so severe in terms of stress on the side wall of a worm tank.

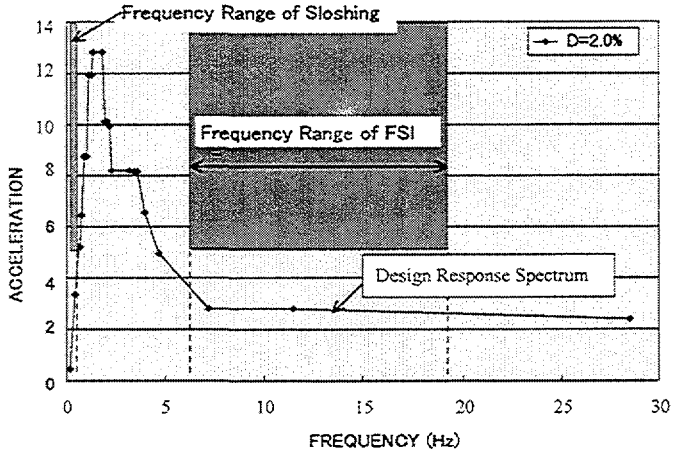

Fig. 15 Comparison of the Frequencies of the worm Tank and Design Spectrum

Stress

The worm tank was not excited at the time of an earthquake. The usual stress except the concentrated stress in an earthquake are same level as that of water pressure. Maximum stress under water pressure appeared at the center of the lower side wall. In the seismic excitation, maximum stress appeared at the column. Maximum stress occurred at deferent part of the worm tank. Except for each side of the column, the stress level of the side wall is below 2 kgf/mm^2. At the side of the column, stress rises above 10 kgf/mm^2. The differences are not so large. The stress level in longitudinal excitation is larger than that of lateral excitation. The stress distribution in the longitudinal excitation is different from that of lateral excitation. The stress in the longitudinal excitation distributed narrowly and that of lateral excitation distributed widely.

The stress in the longitudinal excitation caused by the vibration of the tie-rod and the stress in the lateral excitation by the bending of the column. Using the design criteria of a cylindrical shell, we estimated the buckling load of the worm tank.

$$\sigma_b = 0.4Et/1.5D = 5.5 \text{ kgf/mm}^2$$
$$\sigma_c = 0.9\sigma_y = 18.9 \text{ kgf/mm}^2$$

At the center of the side wall, axial stress is about 2 kgf/mm^2 and hoop stress is 5 kgf/mm^2 . It seems that there was no stress level that exceeded the critical stress.

Local buckling in the vibration test

In the vibration tests conducted in 1996, it was observed that local buckling occurred near the column during lateral excitation. We supposed that it was caused by residual stress due to welding or initial strain under fabrication. In this analysis, stress concentration caused by the vibration of the tie-rod and the bending of the column were observed at the sides of the column. The stresses near the column were five times larger than that of the side wall. In the vibration test, we used a tank model with an uniform thickness. We analyzed a model with uniform thickness. The stress distribution of the worm tank with an uniform thickness were shown in Fig.16 and Fig.17. The effect of the wall thickness on the stress distribution was observed clearly. It was found that the stress level of the tank with an uniform thickness are two times larger than that of actual worm tank. The maximum stress distributed near the center of the span of the column narrowly. On the other hand, the maximum stress of the actual tank appeared at the end of the column as shown in Fig.11. We conducted high level excitation in the test. The stress concentration induced local buckling near the column

part of the side wall. This is a phenomena of the test model tank and not that of the actual tank.

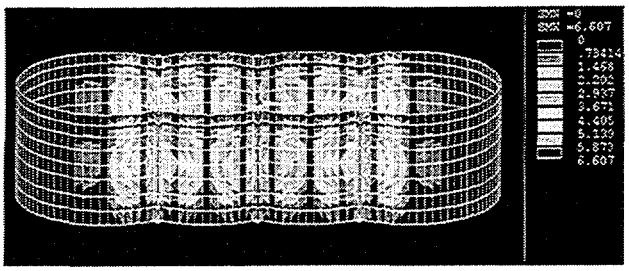

Fig.16 Hoop Stress of the worm tank with uniform thickness in the Lateral Excitation

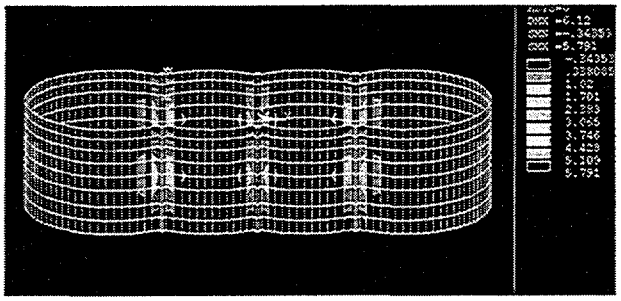

Fig.17 Axial Stress of the worm tank with uniform thickness in the Lateral Excitation

CONCLUDING REMARKS

We conducted a response spectrum analysis of an actual worm tank and the following results were obtained.

1 The frequency range of the sloshing and bulging modes is out of the peak range in the design spectrum of the worm tank.

2 At the joints of the column and tie-rod, peak stress was observed in the longitudinal excitation and that was observed at the middle of the span of the column in the lateral excitation.

REFERENCES

Ogawa N. et. al.,1996, "An Experimental Study of the Sloshing Behavior of the Worm Tank," ASME PVP, Vol.337, 141

Ogawa N. et. al.,1997, "An Experimental Study of the Fluid Structure Interaction Behavior of the Worm Tank," ASME-PVP

Akiyama, H., 1984, " Report on Shaking Table Test of Steel Cylindrical Storage Tank," Journal of High Pressure Gas, vol.21,No.9 (in Japanese)

Abramson and Norman H.,1966, "The Dynamic Behavior of Liquids in Moving Containers," NASA SP-!0&

Kimura K., Takahara H. ,and Sakata M.,1993,"Sloshing in a Rigid Tank Subjected to Pitching Excitation," JSME C-59, 565, 14 (in Japanese)

Kobayashi N. "Impulsive Pressure Acting on the Tank Roofs caused by Sloshing Liquid," Proceedings of 7th WCEE

Akiyama, H.,1989,"Buckling Experiment of Steel Cylindrical Shells subjected to Internal Pressure and Bending-Shear Load, " Transaction of AIJ, vol. 400,(in Japanese)